Cell, Vol. 97, 527–538, May 14, 1999, Copyright ©1999 by Cell Press

p53 Deficiency Rescues the Adverse Effects of Telomere Loss and Cooperates with Telomere Dysfunction to Accelerate Carcinogenesis

Lynda Chin,[1,3,7] Steven E. Artandi,[1,7] Qiong Shen,[1] Alice Tam,[1] Shwu-Luan Lee,[1] Geoffrey J. Gottlieb,[4] Carol W. Greider,[5] and Ronald A. DePinho[1,2,6]

[1]Department of Adult Oncology
Dana-Farber Cancer Institute
44 Binney Street
Boston, Massachusetts 02115
[2]Department of Medicine and Genetics
[3]Department of Dermatology
Harvard Medical School
Boston, Massachusetts 02115
[4]Quest Diagnostics Inc.
Anatomical Pathology
Teterboro, New Jersey 07608
[5]Department of Molecular Biology and Genetics
Johns Hopkins University School of Medicine
Baltimore, Maryland 21205

Summary

Maintenance of telomere length and function is critical for the efficient proliferation of eukaryotic cells. Here, we examine the interactions between telomere dysfunction and p53 in cells and organs of telomerase-deficient mice. Coincident with severe telomere shortening and associated genomic instability, p53 is activated, leading to growth arrest and/or apoptosis. Deletion of p53 significantly attenuated the adverse cellular and organismal effects of telomere dysfunction, but only during the earliest stages of genetic crisis. Correspondingly, the loss of telomere function and p53 deficiency cooperated to initiate the transformation process. Together, these studies establish a key role for p53 in the cellular response to telomere dysfunction in both normal and neoplastic cells, question the significance of crisis as a tumor suppressor mechanism, and identify a biologically relevant stage of advanced crisis, termed genetic catastrophe.

Introduction

Telomeres are nucleoprotein structures that serve a critical function in protecting the ends of linear chromosomes. Maintenance of telomere length and function requires telomerase, a specialized reverse transcriptase, as well as a complex of telomere-associated proteins (van Steensel and de Lange, 1997; van Steensel et al., 1998). Telomerase is comprised of essential catalytic (telomerase reverse transcriptase [TERT]) and RNA components (telomerase RNA [TR]) (reviewed in Greider, 1998). The RNA subunit provides the template for telomere repeat synthesis (Greider and Blackburn, 1989; Yu et al., 1990).

[6]To whom correspondence should be addressed (e-mail: ron_depinho@dfci.harvard.edu).
[7]These authors contributed equally to this work.

Most somatic human tissues and primary cells possess low or undetectable telomerase activity, and telomeres shorten with each cell division in vivo and in vitro. In human cells, a critical telomere length is eventually reached that induces cellular senescence, thus limiting the replicative capacity of cultured cells at the Hayflick limit (Hayflick and Moorhead, 1961). The telomere signal that activates this senescent program operates through the RB and p53 pathways, since cell division beyond the Hayflick limit can occur after antisense neutralization (Hara et al., 1991) or viral oncoprotein inactivation of RB and p53 (Shay et al., 1991). Ectopically expressed hTERT maintains telomere length and allows unlimited growth (Bodnar et al., 1998; Counter et al., 1998; Vaziri and Benchimol, 1998). Thus, telomere shortening in the absence of telomerase plays a critical role in signaling entry into senescence, although immortalization of some epithelial cells requires not only TERT expression but also compromise of the RB pathway (Kiyono et al., 1998).

In primary cells deficient for Rb and p53, continued cellular growth beyond the Hayflick limit results in severe telomere shortening, marked genetic instability, and massive cell death—a period referred to as crisis (Counter et al., 1992). The prominent block to continued proliferation at crisis led to the suggestion that the cell death associated with telomere dysfunction and genetic instability represents a tumor suppression mechanism designed to efficiently eliminate premalignant cells. Although most cells transiting through crisis die, rare survivor cells emerge that can now maintain telomere length through either activation of telomerase or utilization of an alternative pathway thought to involve a recombination-based mechanism (ALT). Such a mechanism has been demonstrated in yeast (Lundblad and Blackburn, 1993; McEachern and Blackburn, 1996). The notion that telomere function may indeed be required for immortalization is supported by the frequent activation of telomerase or ALT in human cancers (Kim et al., 1994; Bryan et al., 1995).

To explore the effect of telomere loss in vivo, telomerase-deficient mice were generated by deletion of the *mTR* gene. Due to the very long telomeres of *Mus musculus*, critical reduction in telomere length and chromosomal instability is only seen following extensive passage of $mTR^{-/-}$ cells (Niida et al., 1998), after successive generations of $mTR^{-/-}$ mice (Blasco et al., 1997; Lee et al., 1998), or in aged $mTR^{-/-}$ organs with high proliferative histories (Rudolph et al., 1999). Telomere shortening and genetic instability in late-generation $mTR^{-/-}$ mice is associated with germ cell depletion in the testis, uterine and intestinal villus atrophy, impaired mitogenic responses of lymphocytes, diminished hematopoietic reserve, and an ulcerative dermatitis. The mechanism underlying organ compromise appears to be apoptosis in most cell types but can involve proliferative defects alone or in combination with apoptosis. The signals and pathways mediating these cellular responses associated with telomere dysfunction have yet to be defined in mammalian cells. In yeast, deletion of critical genes required for telomere maintenance results in telomere shortening and progressive cell death. In addition, the

RAD9-dependent DNA damage checkpoint is induced by a single broken chromosome end (Sandell and Zakian, 1993). The RAD9 and MEC1 DNA damage response pathways in yeast are thought to be similar to the p53 checkpoint in mammalian cells.

Strikingly, as $mTR^{-/-}$ mice advance with age and generation, an increase in cancer incidence is observed presumably due to increased genetic instability caused by telomere shortening, repeated chromosomal fusion-bridge-breakage cycles, and chromosomal loss (Rudolph et al., 1999). These experimental data challenged the simplistic view that telomere dysfunction and genetic instability associated with crisis act as a tumor suppressor. Indeed, the impact of telomere dysfunction on immortalization and tumorigenesis is complex. In cancer-prone mice rendered doubly null for the *INK4a* tumor suppressor and *mTR*, shortened telomeres markedly reduced both cancer incidence and transformation by cellular oncogenes (Greenberg et al., 1999 [this issue of *Cell*]). In contrast, SV40 large T antigen efficiently transformed cells from late-generation $mTR^{-/-}$ mice despite evidence for telomere dysfunction (Blasco et al., 1997; Greenberg et al., 1999). The inactivation of Rb and/or p53 may account for the efficient transformation of cells with significant telomere loss by SV40 large T antigen. These results indicate that the oncogenic potential of a would-be cancer cell bearing short telomeres may depend upon its genetic profile.

The contrasting effect of telomere loss on cellular transformation phenotypes in cells that have intact or inactivated DNA damage pathways suggested that the p53 pathway may alter the cellular response to telomere loss in both normal and neoplastic cells. p53 is a tumor suppressor that serves to protect the cell from a variety of genotoxic and environmental stresses, including DNA damage, hypoxia, nucleotide depletion, and inappropriate growth signals from activated oncogenes. Induction of double strand breaks in DNA by ionizing radiation or genotoxic chemotherapy leads to the rapid stabilization of p53 through phosphorylation of its N terminus (Shieh et al., 1997; Siliciano et al., 1997). This stabilization results in either cell cycle arrest via transcriptional induction of the $p21^{CIP1/WAF1}$ CDK inhibitor or apoptosis (reviewed in Levine, 1997). In senescent human and mouse cells, p53 and $p21^{CIP1/WAF1}$ are coordinately activated, suggesting that there may be overlapping pathways that signal senescence and DNA damage. Here, we examined the functional interactions between telomere dysfunction and p53 in cells and organs of late-generation $mTR^{-/-}$ mice. We found that p53 mediates the adverse effects of critically shortened telomeres. Furthermore, loss of telomere function and p53 deficiency can cooperate to enhance transformation. Our findings underscore the importance of p53 in a pathway that responds to telomere dysfunction and suggest new roles for crisis in cellular transformation.

Results

Critical Telomere Shortening Stabilizes and Activates the p53 Protein

Loss of telomere function in late-generation (G4 onward) $mTR^{-/-}$ mice has been shown to adversely affect the morphology and physiology of diverse cell types and organ systems (Lee et al., 1998; Rudolph et al., 1999). The hypocellularity, abnormal cytoarchitecture, and diminished proliferative potential of these organ systems and cell types are due to a combination of apoptosis and growth arrest. We reasoned that shortened telomeres, exposed chromosomal termini, and/or chromosomal fusion-bridge-breakage events might be recognized as a DNA damage signal and thus activate p53 and its associated checkpoint functions.

To test this hypothesis, the levels and activity of p53 were assessed in primary tissues and cells derived from late-generation $mTR^{-/-}$ mice. Immunoprecipitation and Western blot analysis readily detected p53 in lysates from G6 $mTR^{-/-}$ testis, but not in lysates derived from age-matched $mTR^{+/+}$ testis or from G6 $mTR^{-/-}$ $p53^{-/-}$ littermate controls (Figure 1A). This induction of p53 coincides with the dramatic increase in apoptosis (as assessed by TUNEL) and decreased cellularity in the G6 $mTR^{-/-}$ testis (Lee et al., 1998). Since the role of p53 in DNA damage pathways has been extensively investigated in mouse embryo fibroblasts (MEFs) (Harvey et al., 1993; Lowe et al., 1993; Deng et al., 1995; Kamijo et al., 1997), we assayed p53 protein levels and activity in early-passage MEFs. MEFs from $mTR^{+/+}$ mice and from late-generation $mTR^{-/-}$ mice exhibited marked differences in the proportion of cells expressing p53 as determined by immunohistochemistry. Whereas only 21% of the $mTR^{+/+}$ MEFs at passage 6 stained positive for p53, more than 80% of MEFs derived from G4 and G6 exhibited strong immunoreactivity to p53 (Figure 1B, compare [a] with [b] and [c]).

Activation of p53 involves protein stabilization and posttranslational modifications (Prives, 1998). These modifications allow p53 to activate specific target genes. One of these targets is the CDK inhibitor $p21^{CIP1/WAF1}$, which can induce a G1 or G2 cell cycle block. Endogenous $p21^{CIP1/WAF1}$ levels were increased 3- to 4-fold in late-generation G6 $mTR^{-/-}$ $p53^{+/+}$ MEFs compared to early-generation G2 $mTR^{-/-}$ $p53^{+/+}$ MEFs (Figure 1C). Because G2 $mTR^{-/-}$ and G6 $mTR^{-/-}$ MEFs both lack telomerase activity, we conclude that telomere shortening or associated chromosome fusions and breakage rather than telomerase deficiency per se signals to p53 and accounts for $p21^{CIP1/WAF1}$ induction. As anticipated, $p21^{CIP1/WAF1}$ was not detected in G6 $mTR^{-/-}$ $p53^{-/-}$ cells, indicating that $p21^{CIP1/WAF1}$ induction in $mTR^{-/-}$ cells is largely p53 dependent. To further assess p53 activation, MEF cultures were transfected with pG13CAT, a CAT reporter plasmid containing a multimerized p53-binding site and a minimal TATA box element (Kern et al., 1992). After normalization for transfection efficiency, CAT activity was increased approximately 2-fold in G6 $mTR^{-/-}$ MEFs compared to $mTR^{+/+}$ $p53^{+/+}$ controls at identical passage number (Figure 1D). This activity was strictly dependent upon p53, since $p53^{-/-}$ and G6 $mTR^{-/-}$ $p53^{-/-}$ MEF cultures showed only background levels of CAT activity. Together, these data indicate that critical telomere shortening and the associated chromosomal instability correlate with an increase in the level and the activation of the p53 protein.

Effect of p53 Deficiency on mTR Null Phenotype In Vivo

To determine the effect of p53 loss on mTR phenotypes in vivo, we generated mice doubly null for mTR and p53.

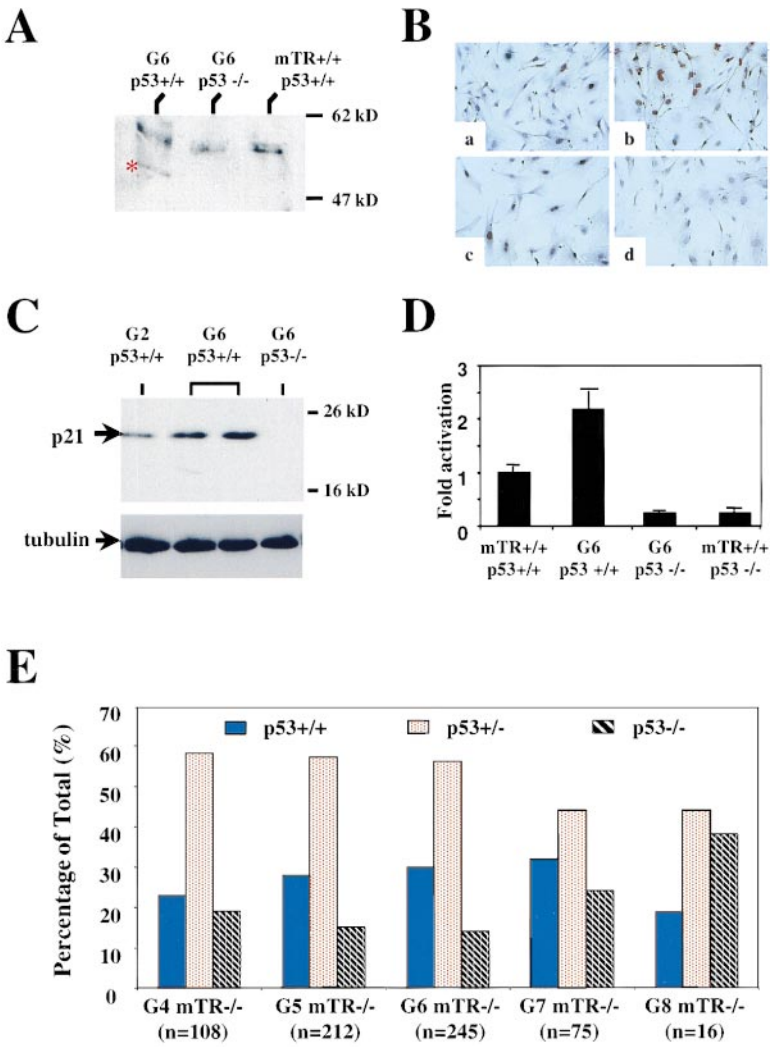

Figure 1. Stabilization and Activation of p53 Protein in Late-Generation mTR-Deficient Testis and MEFs

(A) IP-Western blot assay of testis extract. IP and IB Ab: α-p53. Asterisk indicates location of the p53 band.

(B) α-p53 immunoperoxidase staining of passage 6 MEFs. Increased p53 protein levels as evidenced by an increasing percentage of nuclei exhibiting α-p53 immunoreactivity: (a) $mTR^{+/+}$ MEF, 21% positive; (b) G4 $mTR^{-/-}$ MEF, 82% positive; (c) G6 $mTR^{-/-}$ MEF, 88% positive; (d) negative control, G6 $mTR^{-/-}$ MEF, with no primary antibody. Note the marked senescent morphology of G6 $mTR^{-/-}$ MEFs.

(C) Western blot analysis of early-passage MEF lysates for $p21^{CIP1/WAF1}$ protein. (Top) α-$p21^{CIP1/WAF1}$ antibody. (Bottom) α-tubulin antibody as loading control.

(D) p53-dependent CAT reporter assays documenting activation of p53 protein in G6 $mTR^{-/-}$ MEFs. CAT activities are normalized for transfection efficiency.

(E) p53 genotype distribution of live mice born in successive generations of $mTR^{-/-}$ $p53^{+/-}$ intercrosses expressed as a percentage of all mice within a generation (n = total number). Note increasing percentage of $p53^{-/-}$ mice in G7 and G8.

Successive generational intercrosses were carried out to produce cohorts with progressively shorter telomeres as described previously (Lee et al., 1998; Rudolph et al., 1999). For these matings, the p53 status was maintained in the heterozygous state to avoid potential broad genomic effects arising from p53 deficiency. This mating scheme also produced $p53^{+/+}$ and $p53^{-/-}$ littermate controls for each $mTR^{-/-}$ generation.

Telomere dysfunction results in a dramatic reduction in reproductive competence in late-generation (G6) $mTR^{-/-}$ $p53^{+/+}$ mice (Lee et al., 1998). In the G6 $mTR^{-/-}$ $p53^{+/-}$ intercrosses, we observed an unusually high rate of productive mating pairs (11 of 22 mating pairs) compared to G6 $mTR^{-/-}$ $p53^{+/+}$ matings (Lee et al., 1998), although fertility was still reduced compared to wild-type controls (data not shown). Significantly, we also observed productive matings arising from G7 $mTR^{-/-}$ $p53^{+/-}$ pairs (5 of 17 mating pairs) to yield G8 $mTR^{-/-}$ offspring of all three p53 genotypes. Because p53 heterozygous mice exhibit haploinsufficiency in a number of assays (Gottlieb et al., 1997; Venkatachalam et al., 1998), we speculated that the increased fecundity of the G6 and G7 $mTR^{-/-}$ $p53^{+/-}$ mice could relate to increased survival of germ cells in the $p53^{+/-}$ background.

Previous studies have shown that a small percentage of late-generation $mTR^{-/-}$ embryos experience delayed neural tube closure resulting in diminished litter sizes with advancing $mTR^{-/-}$ generations (Herrera et al., 1999). Moreover, p53 deficiency itself leads to exencephaly in a proportion of females, which accounts for underrepresentation of $p53^{-/-}$ females arising from heterozygous intercrosses (Sah et al., 1995). If p53 deficiency does indeed attenuate the adverse effects of short dysfunctional telomeres, then one might expect to see an overrepresentation of p53 null pups. The genotype distribution of all live mice generated through $mTR^{-/-}$ $p53^{+/-}$ intercrosses was determined at 10 days of age. $p53^{-/-}$ mice were underrepresented as a percentage of total mice in late-generation $mTR^{-/-}$ background (19%, 15%, and 14% for G4, G5, and G6 respectively) (Figure 1E). However, a relative increase in $p53^{-/-}$ mice was evident in G7 and G8 $mTR^{-/-}$ background (24% and 38%, respectively). Since there is progressive telomere shortening and telomere dysfunction in successive generations, mice in G4–G6 were pooled and compared to mice in G7–G8. Significantly, 15% of the G4–G6 $mTR^{-/-}$ mice (86 out of 565 mice) were $p53^{-/-}$ compared to 26% of the G7–G8 $mTR^{-/-}$ mice (24 of 91 mice) ($p = 0.015$ by Fisher's two-sided t test) (Figure 1E). These data indicate that as telomere function worsens in

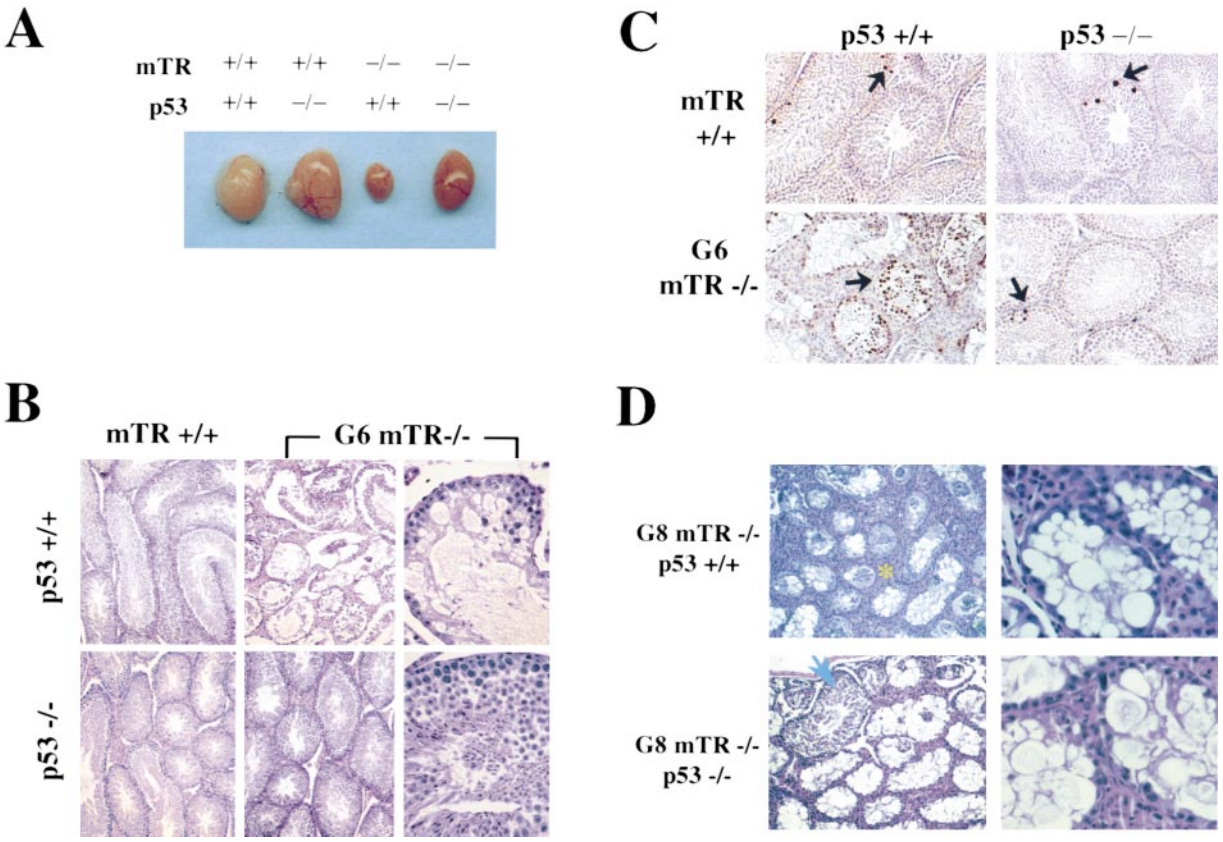

Figure 2. Telomere Dysfunction Induces Germ Cell Depletion by p53-Dependent and Independent Mechanisms

(A) Representative photo of isolated testes from age-matched males with indicated genotypes. Note capsule of $mTR^{+/+}$ $p53^{-/-}$ testis was ruptured accidentally.

(B) Photomicrographs of representative histological sections across seminiferous tubules of testes isolated from age-matched adult males. (Left panel, top) $mTR^{+/+}$ $p53^{+/+}$; (left panel, bottom) $mTR^{+/+}$ $p53^{-/-}$; H&E, 10×. Note p53 deficiency did not alter morphology of the seminiferous tubules. (Middle panel, top) G6 $mTR^{-/-}$ $p53^{+/+}$; (middle panel, bottom) G6 $mTR^{-/-}$ $p53^{-/-}$; H&E, 10×. Note the marked germ cell depletion (manifested as vacuole-like empty space within seminiferous tubules) in G6 $mTR^{-/-}$ $p53^{+/+}$ testis is completely reversed in G6 $mTR^{-/-}$ $p53^{-/-}$ testis (compare top with bottom panel). (Right panel) same samples as middle panel; PAS, 40×. PAS stain reveals that all stages of spermatogenesis are present in the G6 $mTR^{-/-}$ $p53^{-/-}$ testis. Again note marked germ cell depletion in G6 $mTR^{-/-}$ $p53^{+/+}$ testis (compare top with bottom of right panel).

(C) Photomicrographs of representative TUNEL assay for apoptosis in age-matched adult testis. Note dramatic increase in number of TUNEL-positive nuclei in G6 $mTR^{-/-}$ $p53^{+/+}$ testis, which is largely rescued by p53 deficiency in the G6 $mTR^{-/-}$ $p53^{-/-}$ testis. Arrows, TUNEL-positive nuclei.

(D) p53 deficiency does not rescue germ cell depletion in G8 $mTR^{-/-}$ testis. G8 $mTR^{-/-}$ $p53^{+/+}$, H&E, 10×, top left; 40×, top right. G8 $mTR^{-/-}$ $p53^{-/-}$, H&E, 10×, bottom left; 40×, bottom right. Note extensive germ cell loss in both samples. The p53-independent germ cell elimination in G8 $mTR^{-/-}$ testis provides evidence for late crisis in vivo. Arrow shows single tubule with spermatogenesis. Asterisk indicates interstitial hyperplasia.

G7 and G8, $p53^{+/+}$ and $p53^{+/-}$ mice are at a significant survival disadvantage compared to $p53^{-/-}$ mice. These organismal findings prompted a more thorough assessment of how loss of p53 impacts on organ systems adversely affected by telomere dysfunction.

Role of p53 in Germ Cell Apoptosis in Late-Generation *mTR*$^{-/-}$ Testis

Telomere loss in late-generation $mTR^{-/-}$ testis culminates in sterility due to an apoptotic elimination of germ cells (Lee et al., 1998). To determine the impact of progressive telomere dysfunction on testis cellularity and architecture as well as to assess the in vivo relevance of p53 upregulation in this process, testis samples from late-generation $mTR^{-/-}$ mice that were p53 competent (+/+ or +/−) or deficient (−/−) were examined on both macroscopic and microscopic levels. In $mTR^{+/+}$ testis, p53 status did not affect testicular volume or significantly alter the cytoarchitecture of seminiferous tubules (Figures 2A and 2B). In $mTR^{-/-}$ mice, a decrease in testis size that correlated with germ cell depletion by histology was first evident in G5 $mTR^{-/-}$ animals and became more prevalent in G6 $mTR^{-/-}$ mice (Lee et al., 1998). Gross testis size was consistently rescued to near normal in G6 $mTR^{-/-}$ $p53^{-/-}$ mice compared to G6 $mTR^{-/-}$ $p53^{+/+}$ littermates (see Figure 2A for representative comparison). Using a scoring system of normal, 1+, 2+, or 3+ to reflect progressive germ cell depletion and tubular atrophy, we examined in more detail the microscopic changes associated with telomere dysfunction in late-

Table 1. Degree of Germ Cell Depletion in Age-Matched $mTR^{-/-}$ Testes

	$p53^{+/+}$ or $p53^{+/-}$	$p53^{-/-}$
G5 $mTR^{-/-}$	Normal	Normal
	Normal	Normal
	2+ atrophy	Normal
G6 $mTR^{-/-}$	Normal	Normal
	1+ atrophy	Normal
	1+ atrophy	Normal
	2+ atrophy	Normal
	2+ atrophy	1+ atrophy
	3+ atrophy	2+ atrophy
	Normal	2+ atrophy
G7 $mTR^{-/-}$	3+ atrophy	1+ atrophy
	3+ atrophy	1+ atrophy
	1+ atrophy	2+ atrophy
G8 $mTR^{-/-}$	3 + atrophy	1+ atrophy
	3 + atrophy	3+ atrophy

H&E sections of age-matched testis samples were examined and scored as follows: Normal = normal testis histology; 1+ atrophy = <10% of the tubules exhibited atrophy; 2+ atrophy = ~50% of the tubules are abnormal; 3+ atrophy = >90% to total germ cell depletion.

generation $mTR^{-/-}$ mice (Table 1). Most of the G5–G7 $mTR^{-/-}$ $p53^{-/-}$ mice showed improved histology compared to their age-matched controls with competent p53 function. TUNEL assays demonstrated that the restoration of germ cells in the G5–G7 $mTR^{-/-}$ $p53^{-/-}$ testis is accompanied by a dramatic reduction of apoptosis to levels observed in $mTR^{+/+}$ testis (Figure 2C). These findings indicate that germ cell apoptosis coincident with telomere loss is mediated by p53.

As telomere function worsens in later generations of mTR deficiency, germ cell death by p53-independent mechanisms becomes evident. Whereas all G5 $mTR^{-/-}$ $p53^{-/-}$ testes exhibited normal histology, 3 of 7 G6 $mTR^{-/-}$ $p53^{-/-}$ samples still showed varying degrees of pathology (Table 1). Furthermore, p53-independent cell death becomes a more consistent feature in G7 and G8, since all of the five G7–G8 $mTR^{-/-}$ $p53^{-/-}$ testis samples showed significant germ cell depletion microscopically (Figure 2D). Of note, the G8 $mTR^{-/-}$ $p53^{-/-}$ mouse that exhibited a relatively normal histology (1+ germ cell depletion, Table 1) had significantly longer telomere length by flow FISH determination (data not shown) than the other G8 $mTR^{-/-}$ $p53^{-/-}$ mouse. Therefore, cell death in the context of extreme telomere dysfunction, genetic instability, and p53 deficiency in G7 and G8 $mTR^{-/-}$ mice may represent a more accurate model of the late stage of crisis experienced by human cells that bypass senescence (see Discussion).

p53-Dependent Biphasic Arrest in Late-Generation $mTR^{-/-}$ MEF Cultures

Activation of p53 and $p21^{CIP1/WAF1}$ via classical DNA damage stimuli typically results in a block in cell cycle progression. To determine whether telomere loss induces such a block, subconfluent early-passage MEFs were treated with BrdU and labeled with propidium iodide prior to FACS analysis. As shown in Figure 3A, DNA content analyses of G6 $mTR^{-/-}$ $p53^{+/+}$ MEFs revealed a profile consistent with a biphasic block as evidenced by marked accumulation of cells in G1 and G2/M phases. Accordingly, BrdU incorporation assay showed that 36% of the G6 $mTR^{-/-}$ $p53^{+/+}$ cells were in G1 phase, 3% were in S phase, and 40% were in G2/M (Figure 3A, top panel). In contrast, $mTR^{+/+}$ $p53^{+/+}$ MEF cultures demonstrated 35% of cells in S phase and only 13% in G2/M. Consistent with the established role of p53 and $p21^{CIP1/WAF1}$ in mediating a biphasic arrest in response to DNA damage signals (Brugarolas et al., 1995; Deng et al., 1995; Bunz et al., 1998) loss of p53 abrogated this block. Modest attenuation of the cell cycle block was evident in the G6 $mTR^{-/-}$ $p53^{+/-}$ cultures, suggesting functional haploinsufficiency. However, loss of p53 does not appear to eliminate the cell cycle blocks completely, since G6 $mTR^{-/-}$ $p53^{-/-}$ MEFs still exhibited fewer cells in S phase (33% vs. 55%) and more cells in G2/M (14% vs. 7%) than $mTR^{+/+}$ $p53^{-/-}$ MEFs. Thus, both the apoptotic response and cell cycle arrest induced by telomere dysfunction are mediated by p53.

Telomere Length and Cytogenetic Profile in the Absence of p53

To rule out the possibility that p53 status influences telomere metabolism, flow FISH methodology was utilized to determine relative telomere lengths in multiple independent MEF and thymocyte cultures. As shown in Figure 3B, all of the G6 $mTR^{-/-}$ MEF cultures regardless of p53 status exhibited an equivalent and marked decline in mean telomere signal relative to $mTR^{+/+}$ MEFs (75% reduction). Similar results were obtained for primary thymocytes, irrespective of p53 status (Figure 3C).

Telomere shortening in $mTR^{-/-}$ mice results in loss of telomere function and chromosome end-to-end fusion (Blasco et al., 1997; Rudolph et al., 1999). Cells with short telomeres and intact p53-mediated DNA damage responses may be more efficiently "culled" from the population (via apoptosis or arrest); therefore, p53 null cells may accumulate more end-to-end fusions than their $p53^{+/+}$ counterparts. Indeed, analysis of metaphase spreads derived from G6 $mTR^{-/-}$ $p53^{+/+}$ MEFs showed a rate of 0.42 (SD 0.71) chromosomal fusions per metaphase, a rate consistent with previous studies (Figure 3D) (Blasco et al., 1997; Greenberg et al., 1999; Rudolph et al., 1999). By comparison, G6 $mTR^{-/-}$ $p53^{-/-}$ MEFs exhibited 1.65 (SD 2.59) fusions per metaphase, a 3-fold increase ($p = 0.012$). Together, these data indicate that p53 deficiency restores neither telomere length nor function in the telomerase-deficient mouse. The rescue of proliferation, cellularity, and cell death is therefore due to loss of p53 checkpoint functions. Continued proliferation in the absence of the p53 checkpoint may lead to an increased loss of telomere sequences and therefore account for the increased frequency of chromosome fusions.

Tumorigenic Initiation and Progression in the Setting of Telomere Dysfunction and p53 Deficiency

The finding that p53 loss enables survival in the face of telomere dysfunction raised the distinct possibility that

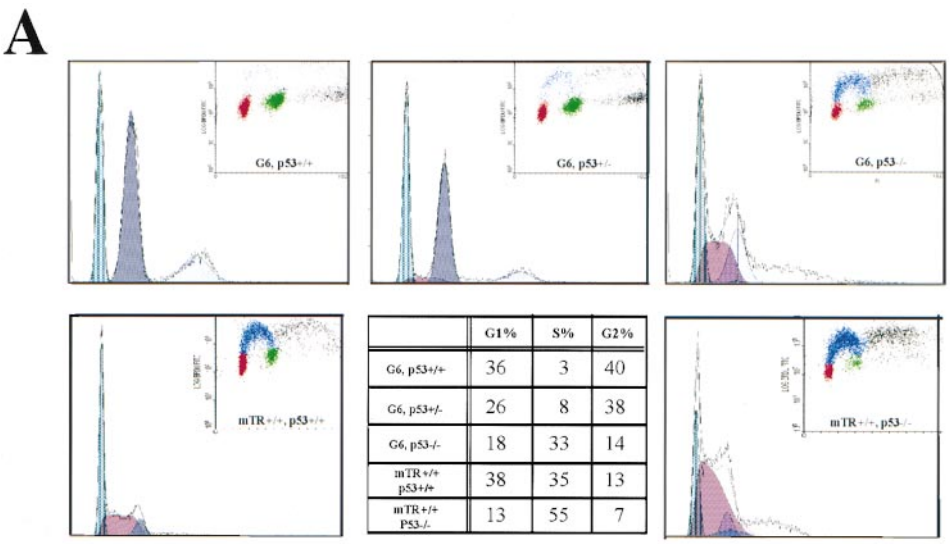

	G1%	S%	G2%
G6, p53+/+	36	3	40
G6, p53+/-	26	8	38
G6, p53-/-	18	33	14
mTR+/+ p53+/+	38	35	13
mTR+/+ P53-/-	13	55	7

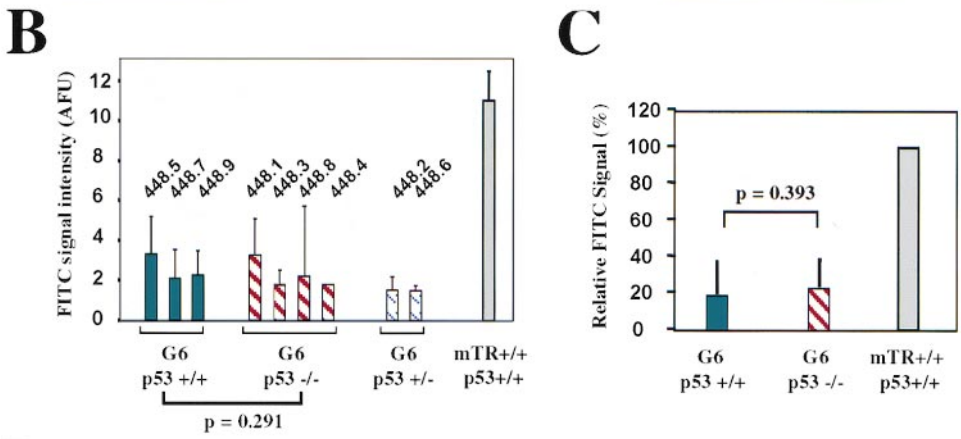

D

	G6 mTR-/- p53+/+ Cultures			G6 mTR-/- p53-/- Cultures		
	448.5	448.7	Total	448.1	448.8	Total
# metaphases	18	8	**26**	17	14	**31**
% aneuploid	44%	75%	**54%**	94%	79%	**87%**
# fusion per metaphase	0.44	0.375	**0.42**	1.24	2.14	**1.65**

p = 0.012

Figure 3. Cell Cycle Analysis, Cytogenetics, and Telomere Lengths in MEFs

(A) Induction of p53-dependent biphasic blocks in late-generation $mTR^{-/-}$ MEFs. Representative cell cycle profile and BrdU incorporation of early-passage (p4) MEFs. Note prominent G2 peaks in G6 $mTR^{-/-}$ $p53^{+/+}$ and G6 $mTR^{-/-}$ $p53^{+/-}$ cultures (representative of five independent cultures examined). Insets: dot plot representations of BrdU incorporation of the corresponding MEF cultures. Red dots represent cells in G1 phase of the cell cycle, green dots represent cells in G2, and blue dots represent cells actively incorporating BrdU. Table: percentage of cells in each phase of the cell cycle according to BrdU incorporation assays.

(B and C) Relative telomere lengths in early-passage G6 $mTR^{-/-}$ MEF cultures (B) or primary thymocytes (C) derived from littermates. Note that telomere lengths are reduced in G6 $mTR^{-/-}$ cells and are not significantly affected by p53 deficiency. For $mTR^{+/+}$ $p53^{+/+}$ MEFs, data are pooled from two independent cultures. Telomere lengths are expressed as mean absolute flouresence units (AFU) minus mean background autoflouresence. For thymocytes, n = 3 mice. p values were calculated by one-tailed Student's t test.

(D) Cytogenetics in two independent MEF cultures was analyzed for both G6 $mTR^{-/-}$ $p53^{+/+}$ and G6 $mTR^{-/-}$ $p53^{-/-}$. Increased chromosomal fusions ($p = 0.012$) and aneuploidy are evident in MEFs from $p53^{-/-}$ littermates.

Table 2. Myc/RAS Transformation Assays with or without Exogenous Telomerase Reconstitution

MEF Culture	Experiment	Avg. Foci Number per 10 cm Plate		Statistics
		Myc/RAS + mTR	Myc/RAS + Vector	
448.1 G6 *mTR*$^{-/-}$ *p53*$^{-/-}$	1	18	33	p = 0.013
	2	20	58	
	3	47	45	
	4	21	55	
	5	62	97	
448.3 G6 *mTR*$^{-/-}$ *p53*$^{-/-}$	2	30	74	p = 0.011
	3	35	97	
	4	12	52	
	5	41	62	
448.4 G6 *mTR*$^{-/-}$ *p53*$^{-/-}$	2	36	47	p = 0.015
	3	20	45	
	4	36	47	
	5	42	94	
448.8 G6 *mTR*$^{-/-}$ *p53*$^{-/-}$	1	1	7	p = 0.038
	2	5	11	
	3	6	17	
	4	26	27	
	5	11	22	
G5 *mTR*$^{-/-}$ *INK4a*$^{-/-}$	5	8	2	ND

Each experiment represents an independent precipitate. Averaged foci counts were obtained by counting two to six 10 cm transfected plates. Foci number generated by Myc/RAS + mTR transfection was taken as 100% in each experiment, and foci count generated by Myc/RAS + vector transfection was calculated as percentage of the Myc/RAS + mTR transfection and plotted in Figure 4A. Statistical analyses were performed using a one-tailed Student's t test.
ND, not determined.

loss of telomere function and the consequent genomic instability could cooperate with p53 deficiency to initiate the process of cellular transformation. To test this hypothesis, we exploited the quantitative Myc/RAS cooperation assay (Land et al., 1983; Mukherjee et al., 1992). This assay allows for development of the malignant phenotype to be observed over time from focus formation to establishment of permanent cell lines to tumor formation in SCID mice. Cotransfections of Myc/RAS plus either an empty plasmid ("vector") or a genomic fragment encoding the *mTR* gene ("mTR") were performed in multiple independent experiments on several independently-derived G6 *mTR*$^{-/-}$ *p53*$^{-/-}$ MEF cultures, and the rates of focus formation were determined (Table 2 and Figure 4A). Transfection of this mTR genomic fragment restored telomerase activity in *mTR*$^{-/-}$ cells (Figure 4B). In contrast to the findings that telomerase reconstitution enhanced focus formation in G5 *mTR*$^{-/-}$ *INK4a*$^{-/-}$ MEFs (Greenberg et al., 1999), we demonstrated that the addition of mTR consistently suppressed the rate of Myc/RAS focus formation in G6 *mTR*$^{-/-}$ *p53*$^{-/-}$ MEFs (Table 2), while restoration of telomerase activity in *mTR*$^{+/+}$ *p53*$^{-/-}$ MEFs had no significant effect (data not shown). These results indicate that telomere dyfunction acts synergistically with p53 deficiency to initiate malignant transformation, presumably by enhancing genetic instability.

Focus formation represents an early step in transformation. To determine the effect of telomere dysfunction on subsequent steps, subcloning efficiency was determined. Despite a lower rate of focus formation, Myc/RAS foci transfected with mTR exhibited a significant enhancement in subcloning efficiency—23 of 26 (89%) mTR foci were successfully established as permanent cell lines compared with only 19 of 32 (59%) vector foci (Figure 4C, p value = 0.018). Similar differences were observed in low-density seeding experiments (data not shown). However, when these established cell lines were injected into SCID mice, mTR lines and vector lines formed tumors with similar efficiency (Figure 4D). Furthermore, the average weight of mTR tumors was not significantly different from that of the vector tumors. Taken together, the differences in the subcloning efficiency of the mTR versus vector cells and their similarity in tumorigenic potential following prolonged passage in culture argue that telomerase provides a significant advantage in steps following the initiation of cellular transformation. However, once telomerase-deficient cells have adapted to the existing telomere dysfunction, they grow as efficiently as telomerase-expressing cells. The mechanisms by which tumorigenic potential is maintained in these late stages of tumorigenesis in the presence of telomere dysfunction remain to be determined.

Discussion

As telomerase-deficient cells traverse replicative senescence via loss of RB/p16^{INK4a} and/or p53/p19^{ARF} or overexpression of Myc, continued telomere attrition results in the loss of chromosomal integrity with consequent genetic instability. The cellular response to this genomic crisis is varied, complex, and poorly understood. Recent results have shown that removing the telomere-binding protein TRF2 from telomeres will directly activate a p53-dependent apoptosis pathway (Karleseder et al., 1999). Whether loss of TRF2 binding, or short telomeres or cycles of fusion-bridge-breakage formation mediate the p53 induction described in this report remains to be

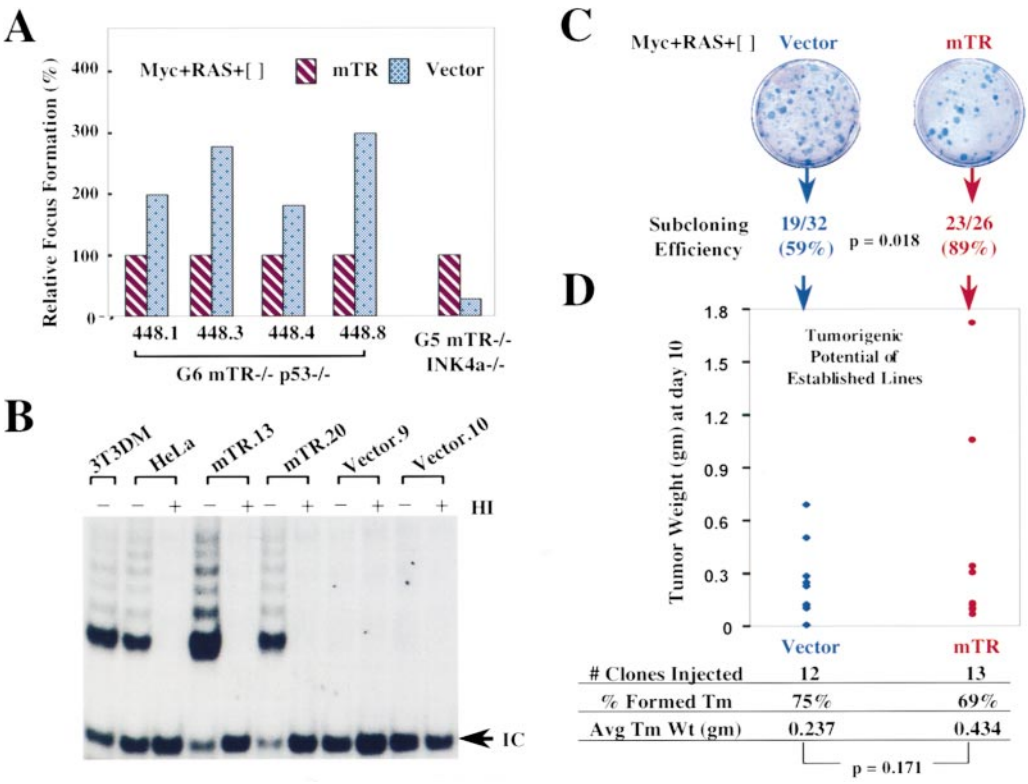

Figure 4. Telomere Dysfunction Can Drive Tumorigenic Initiation but Not Progression

(A) Myc/RAS focus formation of four independent G6 $mTR^{-/-}$ $p53^{-/-}$ MEF cultures. Histograms show relative transformed foci counts derived from transfections that included an "mTR" expression plasmid (red hatched bars) or empty "vector" control (stippled blue bars). Foci counts in Myc+RAS+mTR cotransfection were taken as 100%, and data from five experiments (shown in Table 2) are pooled. For G5 $mTR^{-/-}$ $INK4a^{-/-}$ MEF, p10 culture was used in the same experiment as the G6 $mTR^{-/-}$ $p53^{-/-}$ MEFs.

(B) Telomerase activity is reconstituted by expression of mTR in transformed clones and absent in vector clones. TRAP assay was performed as described previously (Blasco et al., 1997) on extracts from two independent mTR or vector cotransfected Myc/RAS transformed clones. HI, heat inactivation; IC, internal control.

(C) Subcloning efficiency of Myc/RAS transformed G6 $mTR^{-/-}$ $p53^{-/-}$ MEFs was enhanced by mTR compared to vector.

(D) Tumorigenic potential of established subclones was determined by tumor growth in mice. Cells (2×10^6) from each of the 12 Myc+RAS+vector subclones and 13 Myc+RAS+mTR subclones were injected subcutaneously into SCID mice, and tumor weights were measured at day 10 after injection. Scatter plot illustrates distribution of tumor weights from the two groups of transformed clones. Rate of tumor formation is similar in both groups, and the average tumor weight is not statistically different ($p = 0.171$; one-sided Student's t test).

determined. Nevertheless, we have established that p53 plays a key role in the cellular response to telomere dysfunction in vivo in both normal and neoplastic cells, a role that is particularly prominent during the early stages of genomic crisis. Furthermore, this p53-mediated pathway can dramatically affect the consequence of telomere shortening during carcinogenesis.

Telomere Dysfunction Activates a p53-Dependent Checkpoint

The $mTR^{-/-}$ mouse serves as a model to study the consequences of telomere loss in vivo. Similar to well-characterized DNA damage checkpoints, the specific response to telomere dysfunction can be either growth arrest or apoptosis depending upon cell type, p53 pathway status, and physiological context. In male germ cells and lymphocytes, telomere loss elicits a strong apoptotic response, whereas MEFs experience a potent biphasic cell cycle block. In the case of MEFs, this arrest occurs in concert with the stabilization and activation of the p53 protein, evident in p53-dependent reporter assays and activation of $p21^{CIP1/WAF1}$. Moreover, the prominent biphasic cell cycle arrest is also consistent with a p53 mediated checkpoint response and the established role of $p21^{CIP1/WAF1}$ as an inhibitor of both the G1 and G2 phases of the cell cycle. Significantly, loss of p53 rescues the cell cycle arrest in MEFs and the apoptotic elimination of male germ cells. Together these data establish p53 as an important effector in a pathway activated by loss of telomere function.

Crisis: Friend or Foe?

Human cells require inactivation of Rb and/or p53 to bypass the major checkpoint that limits replicative lifespan: cellular senescence. Rb/p53 inactivation allows continued cell division beyond senescence, progressive telomere shortening, and entry into crisis, from which only rare survivors will emerge. Our in vivo and cell culture data suggest that the period defined as crisis in cultured cells can be divided into two phases: "early

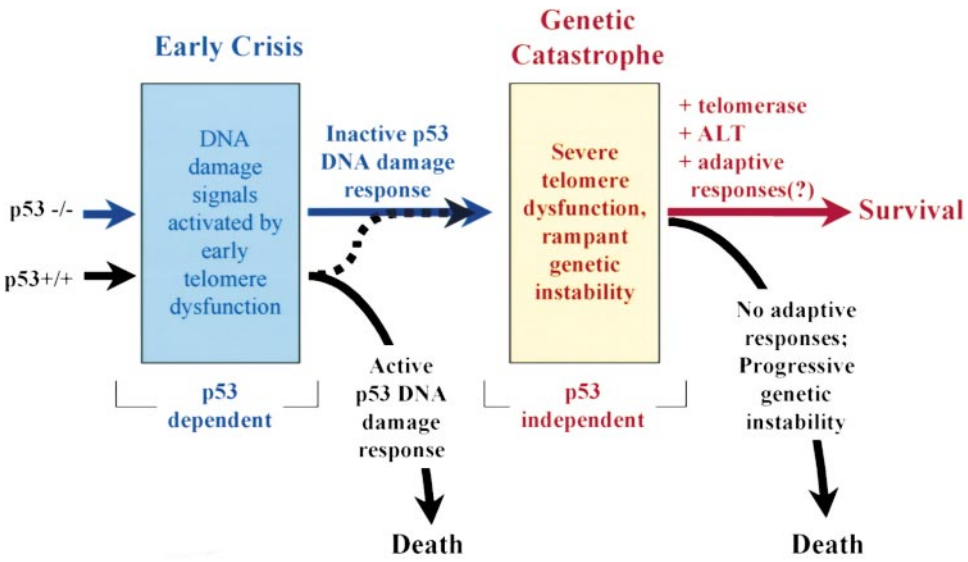

Figure 5. A Model for Crisis and Tumorigenesis

Cell division in the absence of telomerase results in telomere shortening. Oncogene activation or tumor suppressor deletion can facilitate growth beyond senescence, leading to further telomere shortening. In early crisis, p53 is activated, leading to cell death or permanent growth arrest. Inactivation of the p53 DNA damage pathway (dotted black arrow) allows rare cells to continue to divide and bypass the p53 checkpoint. Alternatively, cells that deactivate p53 DNA damage responses early proceed unimpeded through early crisis (blue arrow). Both pathways lead to genetic catastrophe—massive genetic instability in the setting of telomere dysfunction and p53 loss. This results in cell death by p53-independent mechanisms unless cells reestablish telomere maintenance either via telomerase or ALT or develop adaptive responses (red arrow) to tolerate genomic instability.

crisis" and "late crisis," the latter we term "genetic catastrophe" (Figure 5). Cell death in early crisis is p53 dependent. Loss of p53 can circumvent this checkpoint, leading eventually to p53-independent apoptosis, perhaps as a consequence of uncontrolled chromosome fusion-bridge-breakage cycles and progressive genomic instability. Early crisis accounts for efficient germ cell depletion in G6 $mTR^{-/-}$ $p53^{+/+}$, whereas the altered histology of G7 and G8 $mTR^{-/-}$ $p53^{-/-}$ testis provides experimental support for late crisis. Thus, the rampant genetic instability of the G7 and G8 $mTR^{-/-}$ $p53^{-/-}$ cells is associated with loss of cell viability despite p53 deficiency, implying that advanced genomic catastrophe gives way to a p53-independent process.

To understand the interrelationship of crisis, telomeres, and tumorigenic potential, we exploited the multistage features of the MEF cooperation assay. Focus formation is thought to reflect the earliest stages of oncogenic transformation. The ability of exogenous telomerase to reduce focus formation in p53 null cells with short dysfunctional telomeres suggests that genetic instability associated with telomere loss can serve as an engine driving initiation of transformation, but only in the absence of functional p53 (Figure 5). This unanticipated result indicates that telomere dysfunction cooperates with p53 deficiency to facilitate cellular transformation. This finding runs counter to the prevailing view that late crisis represents a second telomere-based block to tumorigenesis in cells that have subverted the senescence checkpoint (Counter et al., 1992). We propose that late crisis is not a checkpoint but instead represents the consequence of unimpeded proliferation in the absence of two powerful genome-stabilizing factors: functional telomeres and p53. Once both telomere function and p53 have been impaired, the fate of the cell is unpredictable and depends on other stochastic genetic changes. Cells that cannot reestablish telomere maintenance or tolerate genomic instability (e.g., germ cells in G7 and G8) will die. In other cells, increased aneuploidy or fusion-bridge-breakage may facilitate genetic changes that promote survival, such as oncogene activation, tumor suppressor deletion, reactivation of telomere maintenance mechanisms, or adaptation to telomere dysfunction (e.g., Myc/RAS-expressing G6 $mTR^{-/-}$ $p53^{-/-}$ MEFs) (Figure 5).

Although loss of telomere and p53 function facilitates initiation of transformation, the reconstitution of telomerase activity greatly improved the capacity of transformed foci to yield immortal cultures. Thus, the activation of telomerase enhances cell survival possibly through avoidance of the p53-independent death of genetic catastrophe (Figure 5). The fact that many human tumors that are telomerase positive still have short telomeres supports the idea that telomerase activation occurs late in tumorigenesis. Together with previous work, our data indicated that, first, during the early stages of tumorigenesis, cells suffer telomere shortening, and second, that telomerase activation is advantageous primarily in later stages of tumorigenesis. The observation that mTR expression facilitates subcloning efficiency of Myc/RAS-transformed late-generation $mTR^{-/-}$ cells supports the importance of telomere maintenance mechanisms during later stages of carcinogenesis.

Telomere Dysfunction, INK4a, and p53

These findings stand in sharp contrast to those obtained from our analysis of mice null for both *mTR* and *INK4a*. In the mTR/INK4a double null mice, loss of telomere func-

tion was associated with a marked reduction in tumor incidence in vivo and a decreased rate of Myc/RAS focus formation in MEFs (Greenberg et al., 1999). Most significantly, in contrast to late-generation $mTR^{-/-}$ $p53^{-/-}$ MEFs, addition of mTR to the Myc/RAS cotransfections of late-generation $mTR^{-/-}$ $INK4a^{-/-}$ MEFs enhanced the rate of focus formation relative to empty vector controls. The $mTR^{-/-}$ $INK4a^{-/-}$ study provides strong in vivo support for the hypothesis that maintenance of telomere function is required for efficient tumorigenesis. $INK4a^{-/-}$ mice lack functional $p19^{ARF}$, a modulator of p53 function activated by inappropiate oncogene activation, but retain intact DNA damage–induced p53 activation (Kamijo et al., 1997). In $mTR^{-/-}$ $INK4a^{-/-}$ mice, it is likely that telomere dysfunction activates p53 via a DNA damage signaling pathway and results in growth arrest or apoptosis, limiting the efficiency of carcinogenesis

The findings of this study may have implications for the use of telomerase inhibitors as an anti-tumor therapy in human cancers. The cooperative interactions of dysfunctional telomeres and p53 deficiency in cancer initiation, together with the capacity for cells to activate ALT, raise questions as to whether telomerase inhibitors would have a beneficial effect in $p53^{-/-}$ tumors. However, in cancer cells harboring intact DNA damage response pathways such as those with an $INK4a^{-/-}$ $p53^{+/+}$ genotype, pharmacological inhibition of telomerase and subsequent telomere shortening would be predicted to be more therapeutically efficacious.

Experimental Procedures

Mating Scheme

$mTR^{+/-}$ mice were mated with $p53^{+/-}$ (Jackson) mice to generate double heterozygotes ($mTR^{+/-}$ $p53^{+/-}$). These mice were intercrossed to generate G1 $mTR^{-/-}$ $p53^{+/+}$, $p53^{+/-}$, and $p53^{-/-}$ animals. All mice are in a mixed genetic background (WW6/C57BL/6), and cousin mating schemes were employed to prevent generation of substrains (Lee et al., 1998). G1 $mTR^{-/-}$ $p53^{+/-}$ mice were mated to generate G2 mice and so on.

Immunoblotting

Testis was dounced in 1% SDS, 20 mM Tris and protease inhibitors and boiled for 5 min. Staph protein A-Sepharose covalently coupled to anti-p53 monoclonal antibody 421 (Oncogene Science) was incubated with 1 mg of extract, washed three times, denatured and subjected to SDS-PAGE, transferred, and probed with a sheep polyclonal anti-p53 (AB7, Oncogene Science). Polyclonal antibody (M-19, Santa-Cruz) was used for analysis of p21 expression in MEFs (30 μg/lane).

Reporter Assay

CAT reporter assays were performed in early-passage MEF cultures as described elsewhere (Pomerantz et al., 1998).

Morphological Analyses and TUNEL Assay of the Testis

Age-matched late-generation $mTR^{-/-}$ $p53^{+/+}$ and $mTR^{-/-}$ $p53^{-/-}$ males were sacrificed and testes dissected for formalin fixation and paraffin embedding. Sections (5 μm) were stained with H&E and PAS. TUNEL assay was performed as described previously (Rudolph et al., 1999) on 3 μm paraffin-embedded sections using the ApoTag-kit (Intergen).

MEF Isolation

G6 $mTR^{-/-}$ mouse embryo fibroblasts (MEFs) were isolated from individual embryos at 13.5 days of gestation from a pregnant G5 $mTR^{-/-}$ $p53^{+/-}$ as previously described (Pomerantz et al., 1998).

Anti-p53 Immunohistochemistry

Early-passage (p6) MEF cultures were fixed in acetone:methanol and blocked in 6% BSA in PBS. Monoclonal anti-p53 antibody (Ab1, Oncogene Science) was diluted 1:500 and incubated on cells overnight at 4°C followed by biotinylated secondary antibody (Vector Laboratories) and streptavidin peroxidase (Vector Laboratories). Diaminobenzidine was used as the final chromogen, and hematoxylin was used as the nuclear counterstain.

MEF Cell Cycle Profiles and BrdU Incorporation Assays

Early-passage MEF cultures were pulsed with BrdU at a final concentration of 10 μM for 3.5 hr. Cells were processed as previously described (Serrano et al., 1997).

MEF Transformation Assay

Expression constructs for c-*myc*, and mutant H-RAS have been described previously (Mukherjee et al., 1992). Early-passage MEFs were cotransfected as described previously (Mukherjee et al., 1992) with 2 μg each of the relevant expression constructs plus 20 μg of genomic DNA as carrier. At 9 to 12 days posttransfection, foci were scored visually and confirmed by microscopic examination to be transformed morphologically. For subcloning efficiency, foci were picked into 48-well plates, then expanded into 10 cm plates. A focus that was capable of growing to confluency in a 10 cm plate was judged to be established. For tumor formation assays, 2×10^6 cells were injected subcutaneously into SCID mice. At day 10, animals were sacrificed, and tumors were weighed.

Telomere Length Analyses

Telomere length determination was performed on early-passage MEF cultures as well as primary thymocytes as described previously (Rufer et al., 1998; Rudolph et al., 1999). Telomere-specific FITC-conjugated $(C_3TA_2)_3$ PNA probe was obtained from PerSeptive Biosystems. Day to day variations in the linearity of the flow cytometer were controlled by the use of FITC-labeled fluorescence beads (Flow Cytometry Standards Corporation). For telomere length determination of MEFs, littermate MEF cultures were assayed simultaneously to reduce experimental variability. At least two independent determinations of the same cultures were performed. For primary thymocytes, age-matched animals were sacrificed, and single-cell suspensions were prepared by mechanical disruption and filtering of thymus tissue. Three independent age-matched sets of animals were used.

Metaphase Spreads

Early-passage MEF cultures were incubated in 0.1 μg/ml colecimid for 1.5 hr then processed as described previously (Rudolph et al., 1999).

Acknowledgments

We are grateful to J. Daley for technical advice on FACS and flow FISH analyses; K.-H. Lee for assistance with MEF isolation; and K. L. Rudolph for the gift of G4 $mTR^{-/-}$ MEFs. The authors thank M. Wong, C. Cohen, and J. Leung for technical assistance with mouse colony management; B. Furman, K. E. Cedeno-Baier, and L. Husted of Quest Diagnostics for tissue sample preparation; N. Schreiber-Agus, T. Raveh, and G. Merlino for critical reading of the manuscript; and members of the DePinho laboratory for helpful comments. This work was supported by grants from the NIH (R01HD34880 and R01HD28317) and an AHA grant-in-aid to R. A. D.; L. C. is supported by an NIH grant (K08AR02104–01). S. E. A. is supported by an NIH grant (5T32CA09172–24) and a Breast Cancer Research Grant Award from the Massachusetts Department of Public Health. A. T. is a Howard Hughes Medical Institute Medical Student Research Training Fellow. C. W. G. is supported by the NIH (CA16519). R. A. D. is an American Cancer Society Research Professor. Support from the DFCI Cancer Core grant to R. A .D. and L. C. is acknowledged.

Received February 17, 1999; revised April 16, 1999.

References

Blasco, M.A., Lee, H.W., Hande, M.P., Samper, E., Lansdorp, P.M., DePinho, R.A., and Greider, C.W. (1997). Telomere shortening and tumor formation by mouse cells lacking telomerase RNA. Cell *91*, 25–34.

Bodnar, A.G., Ouellette, M., Frolkis, M., Holt, S.E., Chiu, C.P., Morin, G.B., Harley, C.B., Shay, J.W., Lichsteiner, S., and Wright, W.E. (1998). Extension of life-span by introduction of telomerase into normal human cells. Science *279*, 349–352.

Brugarolas, J., Chandrasekaran, C., Gordon, J.I., Beach, D., Jacks, T., and Hannon, G.J. (1995). Radiation-induced cell cycle arrest compromised by p21 deficiency. Nature *377*, 552–557.

Bryan, T.M., Englezou, A., Gupta, J., Bacchetti, S., and Reddel, R.R. (1995). Telomere elongation in immortal human cells without detectable telomerase activity. EMBO *14*, 4240–4248.

Bunz, F., Dutriaux, A., Lengauer, C., Waldman, T., Zhou, S., Brown, J.P., Sedivy, J.M., Kinzler, K.W., and Vogelstein, B. (1998). Requirement for p53 and p21 to sustain G2 arrest after DNA damage. Science *282*, 1497–1501.

Counter, C.M., Avilion, A.A., LeFeuvre, C.E., Stewart, N.G., Greider, C.W., Harley, C.B., and Bacchetti, S. (1992). Telomere shortening associated with chromosome instability is arrested in immortal cells which express telomerase activity. EMBO *11*, 1921–1929.

Counter, C.M., Hahn, W.C., Wei, W., Caddle, S.D., Beijersbergen, R.L., Lansdorp, P.M., Sedivy, J.M., and Weinberg, R.A. (1998). Dissociation among in vitro telomerase activity, telomere maintenance, and cellular immortalization. Proc. Natl. Acad. Sci. USA *95*, 14723–14728.

Deng, C., Zhang, P., Harper, J.W., Elledge, S.J., Leder, P.J., and Leder, P. (1995). Mice lacking $p21^{CIP1/WAF1}$ undergo normal development, but are defective in G1 checkpoint control. Cell *82*, 675–684.

Gottlieb, E., Haffner, R., King, A., Asher, G., Gruss, P., Lonai, P., and Oren, M. (1997). Transgenic mouse model for studying the transcriptional activity of the p53 protein: age- and tissue-dependent changes in radiation-induced activation during embryogenesis. EMBO *16*, 1381–1390.

Greenberg, R.A., Chin, L., Femino, A., Lee, K.-H., Gottlieb, G.J., Singer, R., Greider, C.W., and DePinho, R.A. (1999). Short dysfunctional telomeres impair tumorigenesis in the $INK4a^{\Delta 2/3}$ cancer-prone mouse. Cell *97*, this issue, 515–525.

Greider, C.W. (1998). Telomeres and senescence: the history, the experiment, the future. Curr. Biol. *8*, 178–181.

Greider, C.W., and Blackburn, E.H. (1989). A telomeric sequence in the RNA of Tetrahymena telomerase required for telomere repeat synthesis. Nature *337*, 331–337.

Hara, E., Tsurui, H., Shinozaki, A., Nakada, S., and Oda, K. (1991). Cooperative effect of antisense-Rb and antisense-p53 oligomers on the extension of life span in human diploid fibroblasts, TIG-1. Biochem. Biophys. Res. Comm. *179*, 528–534.

Harvey, M., Sands, A.T., Weiss, R.S., Hegi, M.E., Wiseman, R.W., Pantazis, P., Giovanella, B.C., Tainsky, M.A., Bradley, A., and Donehower, L.A. (1993). In vitro gowth characteristics of embryo fibroblasts isolated from p53-deficient mice. Oncogene *8*, 2457–2467.

Hayflick, L., and Moorhead, P.S. (1961). The serial cultivation of human diploid cell strains. Exp. Cell. Res. *25*, 585–621.

Herrera, E., Samper, E., and Blasco, M.A. (1999). Telomere shortening in $mTR^{-/-}$ embryos is associated with failure to close the neural tube. EMBO J. *18*, 1172–1181.

Kamijo, T., Zindy, F., Roussel, M.F., Quelle, D.E., Downing, J.R., Ashmun, R.A., Grosveld, G., and Sherr, C.J. (1997). Tumor suppression at the mouse *INK4a* locus mediated by the alternative reading frame product $p19^{ARF}$. Cell *91*, 649–659.

Karleseder, J., Broccoli, D., Dai, Y., Hardy, S., and de Lange, T. (1999). p53 and ATM dependent apoptosis induced by telomeres lacking TRF2. Science *283*, 1321–1325.

Kern, S.E., Pietenpol, J.A., Thiagalingam, S., Seymour, A., Kinzler, K.W., and Vogelstein, B. (1992). Oncogenic forms of p53 inhibit p53-regulated gene expression. Science *256*, 827–830.

Kim, N.W., Piatyszek, M.A., Prowse, K.R., Harley, C.B., West, M.D., Ho, P.L., Coviello, G.M., Wright, W.E., Weinrich, S.L., and Shay, J.W. (1994). Specific association of human telomerase activity with immortal cells and cancer. Science *266*, 2011–2015.

Kiyono, T., Foster, S.A., Koop, J.I., McDougall, J.K., Galloway, D., and Klingelhutz, A.J. (1998). Both $Rb/p16^{INK4a}$ inactivation and telomerase activity are required to immortalize human epithelial cells. Nature *396*, 84–88.

Land, H., Parada, L.F., and Weinberg, R.A. (1983). Tumorigenic conversion of primary embryo fibroblasts requires at least two cooperating oncogenes. Nature *304*, 596–602.

Lee, H.W., Blasco, M.A., Gottlieb, G.J., Horner, J.W., Greider, C.W., and DePinho, R.A. (1998). Essential role of mouse telomerase in highly proliferative organs. Nature *392*, 569–574.

Levine, A.J. (1997). p53, the cellular gatekeeper for growth and division. Cell *88*, 323–331.

Lowe, S.W., Ruley, H.E., Jacks, T., and Housman, D.E. (1993). p53-dependent apoptosis modulates the cytotoxicity of anticancer agents. Cell *74*, 957–967.

Lundblad, V., and Blackburn, E.H. (1993). An alternative pathway for yeast telomere maintenance rescues est1- senescence. Cell *73*, 347–360.

McEachern, M.J., and Blackburn, E.H. (1996). Cap-prevented recombination between terminal telomeric repeat arrays (telomere CPR) maintains telomeres in Kluyveromyces lactis lacking telomerase. Genes Dev. *10*, 1822–1834.

Mukherjee, B., Morgenbesser, S.D., and DePinho, R.A. (1992). Myc family oncoproteins function through a common pathway to transform normal cells in culture: cross-interference by Max and trans-acting dominant mutants. Genes Dev. *6*, 1480–1492.

Niida, H., Matsumoto, T., Satoh, H., Shiwa, M., Tokutake, Y., Furuichi, Y., and Shinkai, Y. (1998). Severe growth defect in mouse cells lacking the telomerase RNA component. Nat. Genet. *19*, 203–206.

Pomerantz, J., Schreiber-Agus, N., Liegeois, N.J., Silverman, A., Alland, L., Chin, L., Potes, J., Orlow, I., Lee, H.W., Cordon-Cardo, C., and DePinho, R.A. (1998). The *INK4a* tumor suppressor gene product, $p19^{ARF}$, interacts with MDM2 and neutralizes MDM2's inhibition of p53. Cell *92*, 713–723.

Prives, C. (1998). Signaling to p53: breaking the MDM2-p53 circuit. Cell *95*, 5–8.

Rudolph, L., Chang, S., Lee, H.W., Gottlieb, G.J., Blasco, M.A., Greider, C.W., and DePinho, R.A. (1999). Longevity, stress response, and cancer in aging telomerase deficient mice. Cell *96*, 701–712.

Rufer, N., Dragowska, W., Thornbury, G., Roosnek, E., and Lansdorp, P.M. (1998). Telomere length dynamics in human lymphocyte subpopulations measured by flow cytometry. Nat. Biotechnol. *16*, 743–747.

Sah, V.P., Attardi, L.D., Mulligan, G.J., Williams, B.O., Bronson, R.T., and Jacks, T. (1995). A subset of p53-deficient embryos exhibit exencephaly. Nat. Genet. *10*, 175–180.

Sandell, L.L., and Zakian, V.A. (1993). Loss of a yeast telomere: arrest, recovery, and chromosome loss. Cell *75*, 729–739.

Serrano, M., Lin, A.W., McCurrach, M.E., Beach, D., and Lowe, S.W. (1997). Oncogenic ras provokes premature cell senescence associated with accumulation of p53 and $p16^{INK4a}$. Cell *88*, 593–602.

Shay, J.W., Pereira-Smith, O., and Wright, W.E. (1991). A role for both RB and p53 in the regulation of human cellular senescence. Exp. Cell Res. *196*, 33–39.

Shieh, S.Y., Ikeda, M., Taya, Y., and Prives, C. (1997). DNA damage-induced phosphorylation of p53 alleviates inhibition by MDM2. Cell *91*, 325–334.

Siliciano, J.D., Canman, C.E., Taya, Y., Sakaguchi, K., Appella, E., and Kastan, M.B. (1997). DNA damage induces phosphorylation of the amino terminus of p53. Genes Dev. *11*, 3471–3481.

van Steensel, B., and de Lange, T. (1997). Control of telomere length by the human telomeric protein TRF1. Nature *385*, 740–743.

van Steensel, B., Smogorzewska, A., and de Lange, T. (1998). TRF2 protects human telomeres from end-to-end fusions. Cell *92*, 401–413.

Vaziri, H., and Benchimol, S. (1998). Reconstitution of telomerase activity in normal human cells leads to elongation of telomeres and extended replicative life span. Curr. Biol. *8*, 279–282.

Venkatachalam, S., Shi, Y.P., Jones, S.N., Vogel, H., Bradley, A., Pinkel, D., and Donehower, L.A. (1998). Retention of wild-type p53 in tumors from p53 heterozygous mice: reduction of p53 dosage can promote cancer formation. EMBO *17*, 4657–4667.

Yu, G.L., Bradley, J.D., Attardi, L.D., and Blackburn, E.H. (1990). In vivo alteration of telomere sequences and senescence caused by mutated Tetrahymena telomerase. Nature *344*, 126–132.